www.dergipark.gov.tr
ISSN:2148-3736
El-Cezerî Fen ve Mühendislik Dergisi
Cilt: 9, No: 2, 2022 (721-739)

El-Cezerî Journal of Science and Engineering
Vol: 9, No: 2, 2022 (721-739)
DOI: 10.31202/ecjse.997723

ECJSE

Research Paper

Thermodynamic Analysis of a Novel Ammonia Based Direct Steam Generation Trigeneration System

Gamze SOYTURK[1a*], Serpil CELIK TOKER[1b], Onder KIZILKAN[1c]

Isparta University of Applied Sciences, Faculty of Technology, Department of Mechanical Engineering, 32200 Isparta/ Türkiye
gamzeyildirim@isparta.edu.tr

Received/Geliş: 20.09.2021 **Accepted/Kabul:** 06.01.2022

Abstract: The scope of this research is to examine the energetic and exergetic analysis of parabolic trough collector (PTSC) based integrated organic Rankine cycle (ORC) and ejector refrigeration system for generating power refrigeration and hot water. The novel system is driven by solar energy, where the working agent ammonia is directly evaporated while flowing through the parabolic collectors. In addition, a steam-jet ejector refrigeration system working with ammonia again is integrated to utilize the excess heat from the ORC. All the analyses are conducted using Engineering Equation Solver. According to the results of the first and second law analyses, the energetic and exergetic efficiency of the novel trigeneration system is computed as 26.67% and 14.21%, respectively. On the other hand, a parametric analysis was performed to examine the effect of solar irradiation, the temperature at the inlet of the turbine, and generator temperature on combined cycle performance. As stated by the results of the parametric studies of the novel trigeneration system, the energy and exergy efficiency of the multi-purpose energy system and the total exergy destruction rise by the increment of the solar irradiation and temperature at the turbine inlet, while the total exergetic efficiency reduces as the generator temperature rises. Moreover, the highest rate of irreversibility has PTSC with 150 kW, while the lowest amount of irreversibility is calculated as 0.02 kW in the pump of the ejector cooling system.

Keywords: Parabolic trough solar collector, ORC, ejector cooling, ammonia.

Amonyak Bazlı Doğrudan Buhar Üretimli Yeni Trijenerasyon Sisteminin Termodinamik Analizi

Öz: Bu çalışmanın amacı, güç, soğutma ve sıcak su üretmek için parabolik oluklu kollektörlü (PTSC) entegre organik Rankine çevrimi (ORC) ve ejektörlü soğutma çevriminin enerjik ve ekserjetik analizini incelemektir. Trijenerasyon sisteminin performans değerlendirmesini yapmak için EES yazılım programı kullanılmaktadır. Hesaplamalarda termodinamiğin birinci ve ikinci yasaları kullanılmıştır. Termodinamik analiz sonuçlarına göre trijenerasyon sisteminin enerjik ve ekserjetik verimi sırasıyla %26.67 ve %14.21 olarak hesaplanmıştır. Aynı zamanda, güneş ışınımının, türbin giriş sıcaklığının ve jeneratör sıcaklığının kombine çevrim performansı üzerindeki etkisini incelemek için parametrik çalışmalar yapılmıştır. Trijenerasyon sisteminin parametrik çalışmaları incelendiğinde, trijenerasyon sisteminin enerjik- ekserjetik verimi ve toplam ekserji yıkımı, güneş ışınımı ve türbin giriş sıcaklığının artmasıyla artarken, jeneratör sıcaklığının artmasıyla toplam ekserjetik verim azalmaktadır. Ayrıca en yüksek tersinmezlik oranı 150 kW ile PTSC'de iken, en düşük tersinmezlik oranı ise ejektör soğutma sisteminin pompasında 0,02 kW olarak hesaplanmıştır.

Keywords: Parabolik oluklu güneş kolektörü, ORC, ejektörlü soğutma, amonyak

How to cite this article
Soyturk, G., C. Toker, S., Kizilkan, O., *Thermodynamic Analysis of Ammonia Based Direct Steam Generation Trigeneration System* El-Cezerî Journal of Science and Engineering, 2022, 9 (2); 721-739.

Bu makaleye atıf yapmak için
Soyturk, G., C. Toker, S., Kizilkan, O., *Amonyak Bazlı Doğrudan Buhar Üretimi İçin Trijenerasyon Sisteminin Termodinamik Analizi* El-Cezerî Fen ve Mühendislik Dergisi, 2022, 9 (2); 721-739.
ORCID: [a] 0000-0001-7191-8765, [b] 0000-0003-3572-7907, [c]0000-0002-4865-6135

1. Introduction

The energy need is growing in many sectors, containing housing, industry, and transportation [1]. Meeting the majority of the increasing electricity demands from fossil-based fuels causes fast exhaustion of fossil-based resources, global warming, and air pollution [2]. Therefore, many researchers have focused on discovering novel alternative electricity generation from renewable energy resources and excess heat recovery. Solar energy, which is a well-known and most widespread sustainable energy source, is ubiquitous and has a high potential to be utilized [3]. Among the solar energy technologies, PTSC is an important technology for applications of medium and high-temperature ranges especially, poly-generation plants [4]. Today, the PTSCs are well-established solar generation technology with an extensive commercial range. The behavior of the PTSC is significant since the efficiency of the power generation system is based on the performance of the PTSC; thus, many efforts have been paid in order to increase the power system performance and to optimize solar area output [5]. Because the absorber area of the parabolic collector is substantially lower than the collector's gross and aperture areas, water can be heated via the concentration method even at low solar radiation. Several studies on PTC systems have lately been conducted in this area [6]. In the majority of the PTSC systems, synthetic oil, which can operate to temperature ranges of 400 °C, is utilized as a heat transfer medium [5].

ORC is an interesting technology for generating electricity from low-grade solar power systems [7]. The working agent used in ORC is a substantial criterion for the performance of the system. The selection of the working agent to be used in the cycle depends on many quantities, such as the critical temperature, the critical pressure, and the range of the heat source [8]. Besides the thermophysical characteristics of the fluid, environmental effects, for instance, Global Warming Potential (GWP) and Ozone Depletion Potential (ODP) should also be taken into account. From this perspective, the Montreal [9] protocol deals with zero ODP fluids, and the Kyoto Protocol [10] deals with very low GWP fluids. Additionally, the European Union carries out studies to decrease the use of fluorinated gases [11]. As a result, attention in natural fluids with low or zero ODP and GWP values has been rising in recent years. Natural fluids such as carbon dioxide, ammonia, and hydrocarbons haven't effect on the greenhouse effect. Among these fluids, both the ODP value and the GWP value of the natural ammonia fluid are zero, and ammonia has a high latent heat of vaporization. Since the critical temperature of ammonia is 132.41° C, it is widely employed in different organic Rankine cycle applications. For instance, a comparative analysis of the ORC connected to a waste heat-driven Rankine cycle for different fluids including ammonia, isobutane, propane was examined by Ziółkowski et al. [12]. According to the results of their analysis, they stated that the cycle using ammonia as the working agent, which efficiency of the cycle changed between 4% and 16% performed better. Shokati et al. [13] compared system performance using different fluids in an ORC cycle incorporated with a geothermal cycle. They determined the cycle's exergy efficiency for ammonia, n-heptane, and R113 as 51.58%, 50.45%, and 50.97%, respectively.

For the last decades, great amounts of effort have been paid to integrated systems in order to enhance the efficiency of solar-driven power generation plants. One of the most frequently used technologies in integrated systems is the ejector technology [14]. An ejector is a simple and functional device designed to increase the pressure of a secondary stream by directly mixing the energy of the flowing principle fluid's pressure [15]. Zheng and Weng [16] investigated an integrated system of ejector cooling cycle and ORC to generate power and refrigeration. They used R245fa fluid in ORC. While they found the energetic efficiency of the system as 34.1%, they calculated the exergetic performance as 56.8%. Analysis of the low-grade solar-assisted cogeneration system is conducted by Zhang and Mohamed [17]. They concluded from the theoretical analysis that important efforts should be made to improve the cycle efficiency of the cogeneration plant. Khaliq [18] conducted the thermodynamic assessment of the solar-based ejector cooling system. As stated in the research, the highest exergy destruction took place in the solar collectors. Eisavi et al. [19] examined the performance of the new solar-assisted power plant with multiple outputs, including energy generation, heating and refrigerating. The multigeneration system consists of an organic Rankine cycle, absorption cooling cycle working with LiBr-H_2O, and heating process. They stated that using the absorption cooling cycle for the same amount of heat input significantly improves the system performance. Al- Sulaiman et al. [20] examined the performance of the integrated energy plant providing cooling, energy, and heating with the solar parabolic collector for three different solar irradiation operating modes. They also made an exergetic analysis of the same trigeneration system in another paper [21]. Moghimi et al. [22] examined a unique configuration of combined plant involving refrigeration, power, and heating. The combined system is comprised of the Brayton cycle, the Rankine cycle, the ejector cooling system, and the heating process. They examined the energy, exergy, economic and environmental performance of the combined plant. In their results, they stated that the exergetic and energetic efficiency of the integrated plant improved by 7% and 12% in comparison with the basic cycle. Mosaffa and Farshi [23] proposed a new combined system consisting of an ejector cooling system and a heating process. They compared the cycle relating to performance and cost. Besides, optimization of the system has been conducted taking into account the second law efficiency and total cost ratio. Kheiri et al. [24] examined four novel ejector-based ORC systems: basic cycle, with recuperator, with feed liquid heater, and with recuperator and feed liquid. They also compared the performances of the cycles for different working fluids such as R600, R245fa, R236fa. The highest thermal efficiency is achieved in the ORC system with ejector, regenerator, and feed liquid heater when R245fa is used. Gupta et al. [25] examined the integrated sustainable power cycle comprising of a parabolic collector system, ORC, and ejector system. In their results, it was mentioned that the first law efficiency of the plant increased from 12.0% to 13.9% by increasing higher pressure from 800 to 1600 kPa. Khaliq et al. [26] investigated the energetic and exergetic performance of the cogeneration system powered by solar energy. The cogeneration system they examined consists of a parabolic collector, ORC, and ejector absorption cycle. The investigated working agents were R141b, ammonia, isobutane, R143a, and R290 in the ORC and NH_3-$LiNO_3$ fluid couple in the absorption system. They calculated the highest energy and exergy efficiency of the cogeneration system for R141b and the lowest energetic and exergetic performance for R143a. Elakhdar et al. [27] investigated the combined system of parabolic collector supported, ORC, and ejector process to produce refrigeration and electricity from low-grade solar energy. They used R245fa, R141b, R601a, and R123 fluids as working agents in the Rankine cycle. In their study, they calculated the highest entrainment ratio and the highest COP value for the R601a fluid.

Ecological challenges, for instance, climate change, and atmospheric pollution, have become important issues recently. From this perspective, the use of both renewable sources and natural fluids is increasing. In addition, energy problems can be decreased by using renewable energy resources more efficiently. Therefore, multiple production systems such as cogeneration and trigeneration, which provide many useful outputs, become significant. In this study, solar energy-based a new trigeneration system is proposed. The proposed system is incorporated with PTSC, ORC, ejector-based cooling cycle, and domestic hot water preparation process. Ammonia is used in the parabolic trough a solar collector and all sub-systems. As far as we know, no previous research has been investigated the performance assessment of the novel trigeneration power plant with ammonia-based direct steam generation. Unlike the literature, in this study, electricity generation, heating, cooling, and hot water preparation are carried out simultaneously by using natural fluid ammonia in parabolic solar collector, ORC, heating processes, and ejector cooling system. According to most of the literature, synthetic oils are generally employed as the HTF in the PTSC. Direct steam production is a new generation advancement in the field of solar energy. Thanks to direct steam production, high thermal efficiency and low total cost are provided. In addition, direct steam is produced without using heat transfer fluid (HTF) in this paper, unlike the literature. Firstly, the energetic and exergetic analyses are carried out to determine the combined system efficiency. Secondly, parametric analyzes are performed to examine the effect of different parameters on the trigeneration cycle. The principal aims of this research are:

- Suggestion of a solar power-based new trigeneration plant for Isparta city, Turkey.
- Utilization of ammonia, which is an environmentally friendly, natural fluid in all systems that make up the trigeneration cycle.
- Generation of direct steam without using working fluid in the PTSC.
- Production of electricity, refrigerating of space, and hot water preparation from the solar-assisted plant with multiple outputs.
- Determination of energy and exergy performances of the trigeneration cycle.
- Evaluation of the effects of varying different parameters on system performance.

2. System Description

Figure 1. demonstrates the solar-assisted integrated power-refrigeration-hot water generation system schematically. The system includes an ORC in which a PTSC was employed as a boiler, an ejector refrigeration cycle, and a hot water preparation system. Ammonia is employed as the HTF in all systems.

Ammonia is heated to a supercritical condition using a parabolic collector as a heat generator. The ammonia is sent into the turbine, which converts thermal energy into electrical energy. After that, the ammonia leaving the turbine passes from within the three heat exchangers to attain a saturated state. The higher and medium temperature heat exchangers, which are used for heat recovery, are the first and second, respectively, while the condenser is the third. In this study, a generator is used in place of the higher temperature heat exchanger to simulate the ejector refrigeration system. Ammonia gives part of its energy to the ejector cooling cycle. The ammonia is then transferred to a medium-temperature heat exchanger to be used in the production of hot water. Following this, the liquid ammonia condensing in the condenser is pumped back into the higher-pressure state by the pump, resuming the cycle.

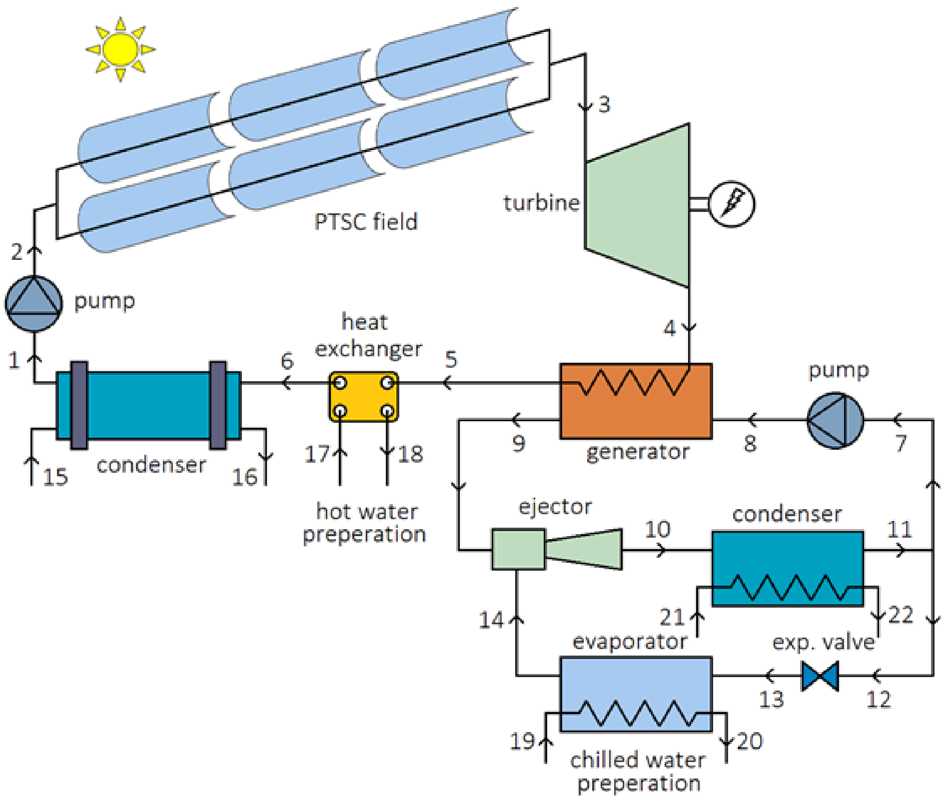

Figure 1. Schematic diagram of ammonia-based PTSC driven trigeneration cycle.

The ejector refrigeration cycle occurs between flows 7 and 14. The excess heat energy of the power cycle is utilized to power the ejector refrigeration cycle. With flow 9, the higher-pressure main fluid enters the ejector. The low-pressure secondary fluid at the evaporator's exit is subsequently drawn to the ejector with flow 14. In the ejector, these two fluids are combined. With flow 10 is transported, this combined flow to the condenser. After that, the heat transfer fluid is condensed into a liquid to remove excess heat. With flow 11 is divided the condensed liquid into two, which are subsequently transferred to two distinct components. Flow 12 delivers a part of the condensed liquid to the expansion valve. Flow 13 then transports it to the evaporator to gain refrigeration capacity. The liquid that remained after condensation enters the pump again with flow 7 by raising the pressure. Finally, the condensed, pressurized liquid is pumped to the generator.

3. Methodology

In this chapter, an explanation of the thermodynamic analysis utilized in this study is presented. Energetic and exergetic analyses are performed using the Engineering Equation Solver (EES) [28] program for the performance assessment of the system. In the current study, the performance assessment is conducted in accordance with the assumptions given below:

- The steady-state operation for all system components.
- Changes in kinetic and potential energies are disregarded.
- The heat losses to/from the pump and turbine are ignored.
- The pressure drops throughout the system are ignored.

In addition, the following assumptions were taken into account in the analysis of the cooling system:

- The fluid is assumed to be saturated liquid at the condenser exit.
- The fluid is assumed to be saturated vapor at the evaporator outlet.
- The fluid is assumed to be saturated vapor at the generator exit.
- The pressure is assumed to be constant during the mixing operation in the ejector.

The calculation method of the parabolic collector, which is the energy source of the integrated plant, basically depends on the reference Kalogirou [4]. Solar irradiation heats the working fluid that passes throughout the receiver after it is reflected by a parabolic collector. To this aim, the working fluid absorbs a substantial quantity of solar energy. The following formulas can be used to compute the convective heat loss between the tube's surface of outer and the environment:

$$h_{c,c-a} = Nu_{air}\, k_{air}/D_g \tag{1}$$

$$Nu_a = 0.4 + 0.54\, Re_{air}^{0.52} \quad \text{for} \quad 10^{-1} < Re < 10^3 \tag{2a}$$

$$Nu_a = 0.3 Re_{air}^{0.6} \quad \text{for} \quad 10^3 < Re < 5 \times 10^4 \tag{2b}$$

where, k, Nu, D_g, and Re are thermal conductivity, Nusselt number, the diameter of the glass cover, and Reynolds number, respectively.

The other part of the heat transfer among environment and cover is the radiation heat transfer in which is determined through the below equation:

$$h_{r,c-a} = \varepsilon_g\, \sigma \left(T_g + T_a\right)\left(T_g^2 + T_a^2\right) \tag{3}$$

Here σ and ε_g demonstrate the Stefan–Boltzmann constant and glass cover's emissivity. The heat transfer from the receiver tube to the glass cover ($h_{r,r-c}$) is calculated as follows:

$$h_{r,r-c} = \frac{\sigma(T_r + T_g)(T_r^2 + T_g^2)}{\frac{1}{\varepsilon_r} + \frac{A_r}{A_g}\left(\frac{1}{\varepsilon_g} - 1\right)} \tag{4}$$

Here T_r, T_g, ε_r, A_g and A_r the show, temperatures of the receiver, the temperature of the glass cover, the emissivity of the receiver, glass cover area, and receiver area, respectively.

Due to the fact that only T_g is unknown among all of the above-mentioned parameters, and given the close relationship between glass and environment temperatures, the parameter should be gained from an energetic balance for glass cover while ignoring the irradiation heat transfer among the environment and the glass cover:

$$T_g = \frac{A_r\, h_{r,r-c}\, T_r + A_g\,(h_{r,c-a} + h_{c,c-a})\, T_a}{A_r\, h_{r,r-c} + A_g\,(h_{r,c-a} + h_{c,c-a})} \tag{5}$$

It should be noted that due to the evacuated space inside the tube, the convection heat transfer operation is disregarded. The overall heat loss coefficient of the collector's (U_L) is estimated using the below formula [4].

$$U_L = \frac{1}{\left[\frac{A_r}{(h_{c,c-a} + h_{r,c-a})A_g} + \frac{1}{h_{r,r-c}}\right]} \tag{6}$$

The useful energy is defined as below:

$$\dot{Q}_u = F_R\left[S\, A_{ap} - A_r U_L (T_{in} - T_a)\right] \tag{7}$$

Here F_R is collector heat removal factor, S is the solar irradiation, A_{ap} is the aperture area of the collector, Ar A_r is the receiver area, T_{in} is the inlet temperature of the working fluid, and T_a is the atmospheric temperature. F_R is calculated from the below equation:

$$F_R = \frac{\dot{m}c_p}{A_r U_L}\left[1 - \exp\left(-\frac{U_L F' A_r}{\dot{m}c_p}\right)\right] \tag{8}$$

here c_p shows the specific heat working fluid, $\dot{m}$ is the mass flow rate of heat transfer fluid and F' represents collector efficiency factor which should be estimated as follow:

$$F' = \frac{U_0}{U_L} \tag{9}$$

here U_0 shows the overall heat loss coefficient between environment and heat transfer fluid calculated from the following equation:

$$U_0 = \frac{1}{\frac{1}{U_L} + \frac{D_o}{h_{fi} D_i} + \left(\frac{D_o \ln\left(\frac{D_o}{D_i}\right)}{2k}\right)} \tag{10}$$

In Eq. (10) D_o, D_i, k and h_{fi} are outer and inner diameters of the receiver tube, thermal conductivity and convection the heat transfer coefficient. For the working fluid, h_{fi} is estimated with the below equation [29]:

$$h_{fi} = \frac{Nu_{fi}\, k_{fi}}{D_i} \tag{11}$$

$$Nu_{fi} = 0.023\, Re^{0.8}\, Pr^{04} \quad \text{for} \quad Re > 2300 \tag{12a}$$

$$Nu_{fi} = 4.364 \quad \text{for} \quad Re < 2300 \tag{12b}$$

Also, the useful heat from the collector can be found from the other formula given in the below:

$$\dot{Q}_u = \dot{m}c_p(T_{out} - T_{in}) \tag{13}$$

here T_{out} is the outlet temperature of the working fluid.

For the performance analysis of the combined solar system, the conservation of mass principle and the laws of thermodynamics are applied to every system element.

The general mass balance equation should be given as below:

$$\sum \dot{m}_{in} = \sum \dot{m}_{out} \tag{14}$$

where, $\dot{m}$ shows the mass flow rate. The energetic balance equilibrium is given below:

$$\dot{Q} + \sum \dot{m}_{in}h_{in} = \dot{W} + \sum \dot{m}_{out}h_{out} \tag{15}$$

In the above equation, $\dot{Q}$ denotes heat retes, $\dot{W}$ shows work, and h is the specific enthalpy.

The exergetic balance equation for the second law analysis of the steady-state system in the can be written as [30]:

$$\dot{E}x_Q - \dot{E}x_W = \sum \dot{m}_{out}e_{out} - \sum \dot{m}_{in}e_{in} + \dot{E}x_{dest} \tag{16}$$

where, $\dot{E}x_Q$ is exergy of heat and $\dot{E}x_W$ is the exergy work, respectively, e is the specific exergy and $\dot{E}x_{dest}$ is exergy destruction. In the above equation, exergies of heat and work and entropy generation rate are given below [31]:

$$\dot{E}x_{dest} = T_0\dot{S}_{gen} \tag{17}$$

$$\dot{E}x_Q = \dot{Q}\,(1 - \frac{T_0}{T}) \tag{18}$$

$$\dot{E}x_W = \dot{W} \tag{19}$$

The specific exergy can be calculated as:

$$e = (h - h_0) - T_0(s - s_0) \tag{20}$$

Where $h_0$and s_0 show the enthalpy and entropy of reference conditions. In addition, the exergy of the sun should be calculated as follow:

$$\dot{E}x_{solar} = SA\left(1 + \frac{1}{3}\left(\frac{T_0}{T_{sun}}\right)^4 - \frac{4}{3}\left(\frac{T_0}{T_{sun}}\right)\right) \tag{21}$$

Here, T_{sun} is the sun's temperature and is taken as 5739 K [32].

The energy and exergy efficiencies should be calculated below:

$$\eta_{en} = \frac{\dot{m}_3(h_3 - h_4) - \dot{m}_2(h_2 - h_1) + \dot{m}_5(h_5 - h_6) + \dot{m}_{14}(h_{14} - h_{13})}{\dot{m}_2(h_3 - h_2)} \tag{22}$$

$$\eta_{ex} = \frac{\dot{m}_3(h_3 - h_4) - \dot{m}_2(h_2 - h_1) + (\dot{m}_{20}\dot{e}_{20} - \dot{m}_{19}\dot{e}_{19}) + (\dot{m}_{18}\dot{e}_{18} - \dot{m}_{17}\dot{e}_{17})}{\dot{m}_2(h_3 - h_2) * (1 - \frac{T_0}{T_{sun}})} \tag{23}$$

After performing thermodynamic assessment of the system in order to evaluate the system performance, it is necessary to conduct a calculation methodology for the investments costs and payback period. Financial evaluation is the foremost feature of an engineering design. With the help of the economic assessment, it becomes easier to judge the feasibility of the project if it is feasible or not. There are several methods to conduct this evaluation. One of the easiest even so useful reference is determination of the payback period [33]. In order to determine the payback period, the initial investment cost of the system should be calculated. For the capital cost calculation, the equations given in Table 1 are used.

Table 1. The cost functions of the system elements

Elements	Function	Reference
PTSC	$C_{PTSC} = 170(A_{ap})$	[34]
HTF	$C_{HTF} = 70(A_{ap})$	[34]
Turbine	$C_{tur} = 6000(\dot{W}_{tur})^{0.7}$	[35]
Pump (ORC)	$C_{pump,ORC} = 3540(\dot{W}_{pump})^{0.71}$	[36]
Condenser (ORC)	$C_C = 516(A_C)^{0.6}$ $A_C = \frac{\dot{Q}_C}{U_C LMTD_C}$ $U_C = 0.15\ W/m^2K$	[37]
Heat exchanger	$C_{Hex} = 1773\dot{m}_{17}$	[36]
Generator	$C_G = 1010(A_G)^{0.8}$ $A_G = \frac{\dot{Q}_G}{U_G LMTD_G}$ $U_G = 0.88\ W/m^2K$	[37]
Ejector	$C_{ejector} = 15960\dot{m}_9\left(\frac{(T_9+273)}{\frac{P_9}{1000}}\right)^{0.05}\left(\frac{P_{10}}{1000}\right)^{-0.75}$	[37]
Condenser (Refrigeration)	$C_C = 516(A_C)^{0.6}$ $A_C = \frac{\dot{Q}_C}{U_C LMTD_C}$ $U_C = 0.15\ W/m^2K$	[37]
Pump (Refrigeration)	$C_{pump,ref} = 200(\dot{W}_{Pump,ref})^{0.65}$	[37]
Expansion valve	$C_{Exp} = 37\left(\frac{P_{12}}{P_{13}}\right)^{0.68}$	[37]
Evaporator	$C_E = 309.14(A_E)^{0.85}$ $A_E = \frac{\dot{Q}_E}{U_E LMTD_E}$ $U_E = 0.2\ W/m^2K$	[37]

4. Results and Discussions

Thermodynamic assessment of the integrated ammonia-based Rankine cycle and ejector refrigeration cycle hot water preparation system was conducted. The system was driven by solar energy by means of parabolic trough solar collectors. As mentioned previously, calculations were performed using EES software [28]. During the analysis, the assumed operating parameters of the proposed system were tabulated in Table 2. The performance assessment of the novel system was investigated for three different cases. At first, analysis was conducted for base conditions using the assumed parameters given in Table 2. Secondly, the hourly performance of the system was examined for four different typical days of the different seasons of a year. Finally, parametric analyses were carried out in order to determine the effects of varying system parameters on the cycle performance.

Table 2. Basic design parameters of the system

Design Parameters	Values
Reference Temperature (℃)	20
Reference Pressure (kPa)	101.325
PTSC [38]	
Solar radiation (W/m^2)	750
Collector lenght (m)	35
Aperture width (m)	4.2
Receiver outside diameter (m)	0.045
Receiver inside diameter (m)	0.04
Glass cover diameter (m)	0.075
Receiver emissivity (-)	0.92
Glass cover emissivity (-)	0.87
Tube thermal conductivity (W/mK)	25
Receiver temperature (℃)	140
Inlet fluid temperature to PTSC (℃)	35
Organic Rankine Cycle [39]	
Turbine isentropic efficiency (-)	0.92
Pump isentropic efficiency (-)	0.85
Condenser temperature (℃)	35
Pressure ratio (-)	3.5
Heat exchanger effectiveness	0.60
Ejector Refrigeration Cycle [40]	
Generator temperature (℃)	95.5
Pump isentropic efficiency (-)	0.88
Ejector entrainment ratio (-)	0.44468

The calculated thermodynamic data for each state point of the integrated system are listed in Table 3. As mentioned previously, the primary analysis was conducted for the assumed parameters by taking the reference temperature 20 °C and reference pressure 101.325 kPa. By utilizing the system operating parameters for the solar-assisted direct steam generated integrated system, the net power production of the ORC was determined as 27.17 kW, while the refrigeration and hot water capacities were calculated to be 12.39 kW and 16.35 kW, respectively. It must be noted that all these calculations were performed for a solar irradiation intensity of 750 W/m^2. The energetic efficiency of the overall cycle was found to be 26.67%. Furthermore, the energy efficiency of the ORC alone was found to be 12.96 %. A similar result was reported by Kajurek et al. [39] in their comprehensive article about the comparative study of ORC working fluids. In their study, they compared the performance of the ORC for different working fluids, and the best result was obtained for ammonia with an energy efficiency of 9.93 %.

According to the results of the exergy analysis, the exergy irreversibility rate of the integrated system was obtained to be 165.6 kW, in which the highest portion with 150 kW of this amount belongs to PTSC. This higher amount is due to the temperature difference between the temperature of the sun and the ambient. In Figure 2, the relative exergy irreversibility rates were given for the base conditions for each system component of examined trigeneration system. It can be seen from the figure that the percentage of the highest destruction contributor is almost 91 % of the destruction.

Table 3. Thermodynamic property value of trigeneration system

State	Fluid	T [°C]	P [kPa]	$\dot{m}$ [kg/s]	h [kJ/kg]	s [kJ/kgK]	e [kJ/kg]	$\dot{E}x$ [kW]
0	R717	20	101.3	-	1536	6.565	-	-
0	water	20	101.3	-	83.93	0.2962	-	-
1	R717	35	1351	0.12	366.1	1.567	295.6	35.47
2	R717	36.23	4728	0.12	373	1.57	301.4	36.17
3	R717	289.2	4728	0.12	2120	6.139	709	85.08
4	R717	185.2	1351	0.12	1887	6.27	437.4	52.49
5	R717	95.99	1351	0.12	1662	5.724	372.5	44.7
6	R717	46.6	1351	0.12	1526	5.327	352.7	42.32
7	R717	35	1351	0.02514	366.1	1.567	295.6	7.43
8	R717	36.48	5722	0.02514	374.5	1.57	303.1	7.618
9	R717	95.5	5722	0.02514	1448	4.555	501.3	12.6
10	R717	35	1351	0.03637	1454	5.099	348.6	12.68
11	R717	35	1351	0.03637	366.1	1.567	295.6	10.75
12	R717	35	1351	0.01123	366.1	1.567	295.6	3.32
13	R717	7	554.1	0.01123	366.1	1.594	287.7	3.231
14	R717	7	554.1	0.01123	1469	5.531	236.5	2.657
15	Water	20	101.3	1.639	83.93	0.2962	0	0
16	Water	40.3	101.3	1.639	168.8	0.5762	2.81	4.605
17	Water	20	101.3	0.09772	83.93	0.2962	0	0
18	Water	60	101.3	0.09772	251.2	0.8311	10.47	1.023
19	Water	24	101.3	0.2693	100.7	0.3529	0.1131	0.03046
20	Water	13	101.3	0.2693	54.64	0.1951	0.3553	0.09568
21	Water	20	101.3	0.8697	83.93	0.2962	0	0
22	Water	30.88	101.3	0.8697	129.4	0.4486	0.8242	0.7169

In the absence of PTSC, the highest exergy irreversibility was calculated in the turbine with 29%. The second law efficiency of the overall system was calculated as 14.21%, which is relatively acceptable. Yamaguchi et al. [41] performed an experimental study about the solar-assisted transcritical Rankine cycle. They utilized evacuated tube solar collectors in order to provide the necessary heat energy for the cycle, and according to their results, about 72 % of the total exergy irreversibility was due to solar collectors.

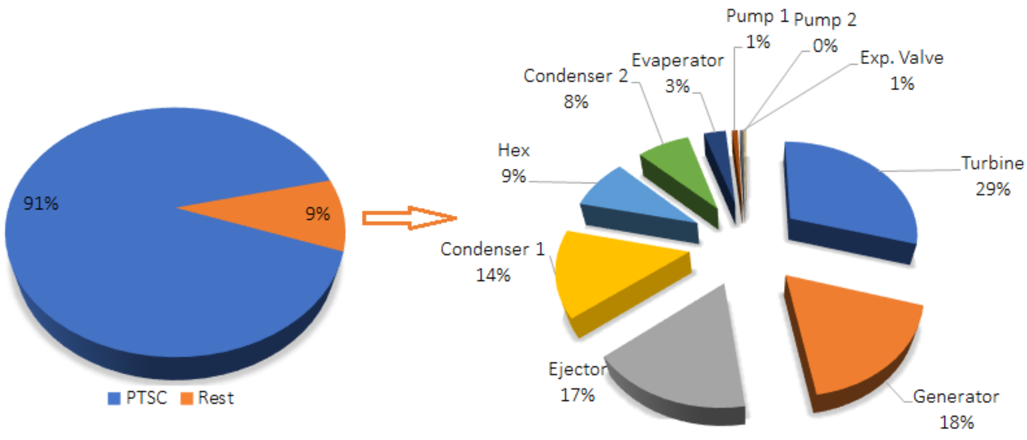

Figure 2. Exergy irreversibility rate of the whole elements of the trigeneration system

In order to investigate the hourly performance of the system, hourly solar radiation data of Isparta were obtained from Photovoltaic Geographical Information System from the Joint Research Centre (JRC) of the European Union [42]. For the analysis, the data were selected randomly in order to simulate the conditions of four different seasons. The data of 16 February 2008 was used for the simulation of the winter season, while the other randomly selected days were 15 May 2015 for spring, 15 August 2011 for summer, and 08 November 2014 for the winter season. Figure 3 shows the hourly variation of ambient temperature and solar irradiation for four different days of the seasons. According to Figure 3a, the highest temperature was recorded to be 29.6 °C for August, followed by 19 °C for May, 15.6 for November, and 5 °C for February.

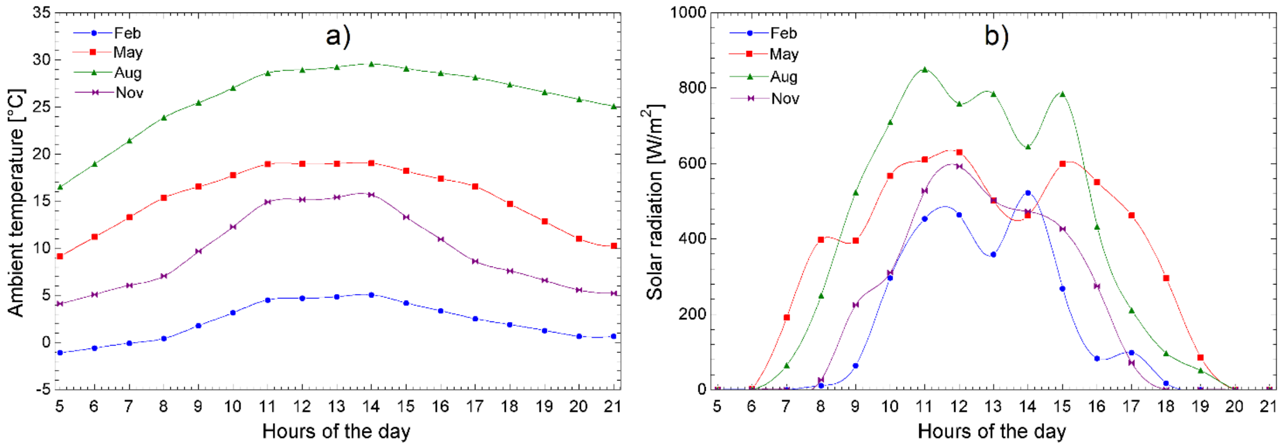

Figure 3. Hourly variation of a) ambient temperature b) solar radiation for Isparta [42]

In Figure 3b, the solar radiation data were plotted against hours of the day. In the early morning of the month of August, the sun rises at about 6 o'clock, and the radiation increases to its maximum value at about 11. At this time, the recorded radiation is 850 W/m^2. As can be seen from the data for all days, there are some sudden changes in the amount of solar radiation due to clouds. In order to reflect the actual case conditions, these data were used instead of average yearly values.

The results of the useful outputs of the solar-driven integrated system were given in Figure 4 for four different typical days of the year. As expected, the maximum net power generation, refrigeration effect, and hot water preparation rate were obtained in August. For this month, the net power generation of the turbine was reached an amount of 21.88 kW at noontime. At this moment, the refrigeration capacity of the ejector refrigerating system was calculated to be 4 kW, while an amount of hot water generation capacity was obtained as 13.86 kW. As expected, for the month of February, the lowest capacity rates were obtained due to the lower radiation intensities. It must be noted that, for all conditions, the operation of the system was assumed to be started after the solar radiation rate of 300 W/m^2. In other words, the solar radiation amount of 300 W/m^2 was taken as the minimum value for the system operation.

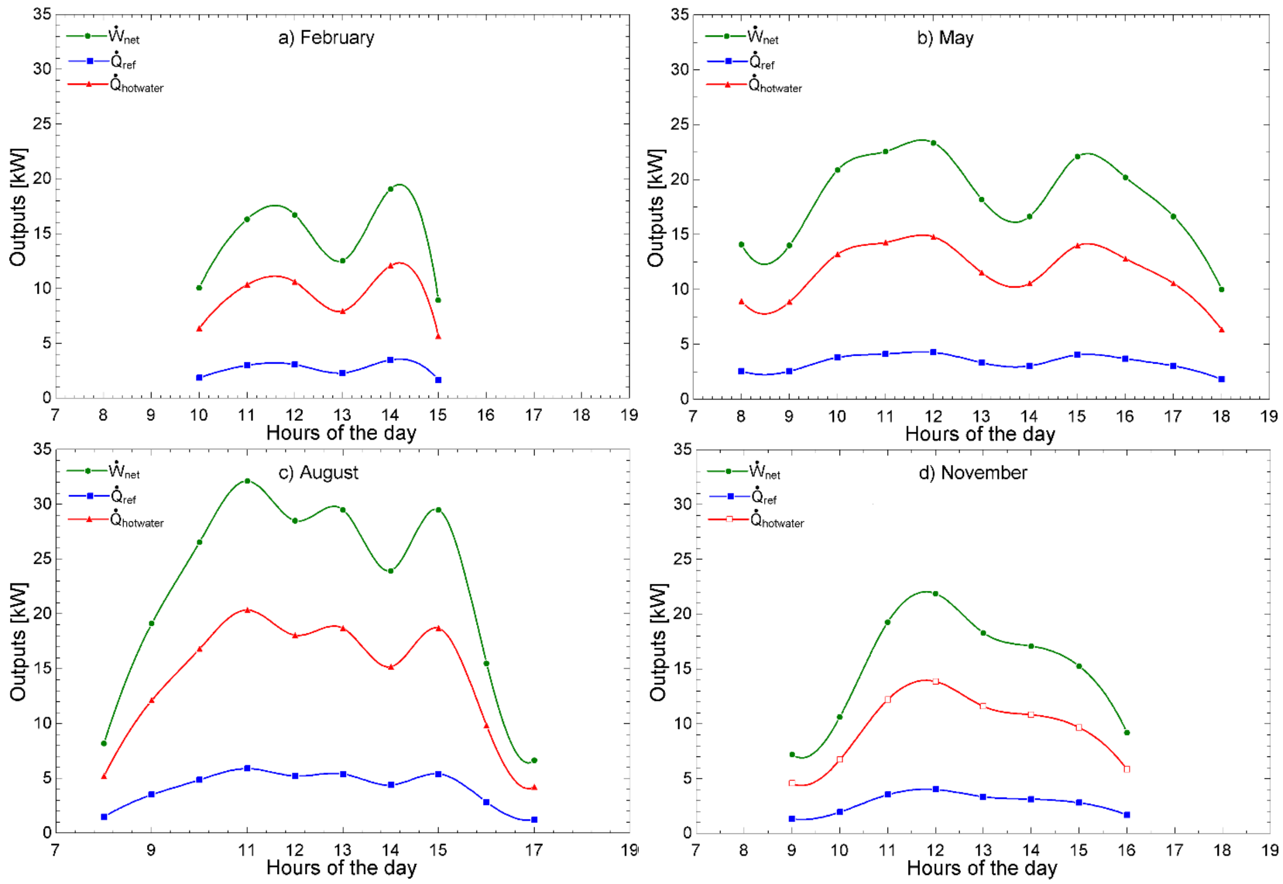

Figure 4. Hourly variation of useful system outputs for the different days of four seasons

At the final part of the study, parametric analyses were carried out by varying the essential system parameters in order to determine the effect of these parameters on the cycle performance. Figure 6 shows that as the solar radiation increases, useful outputs produced by the integrated system per unit time increase. The reason for this increasing trend is that the temperature of the fluid leaving the solar collector rises with the increase in solar radiation, and the production of electricity, cooling, and hot water increases linearly.

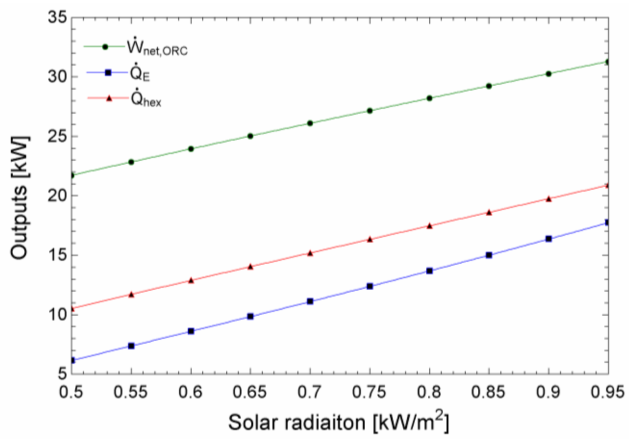

Figure 6. Impact of solar radiation on power generation, cooling, and heating

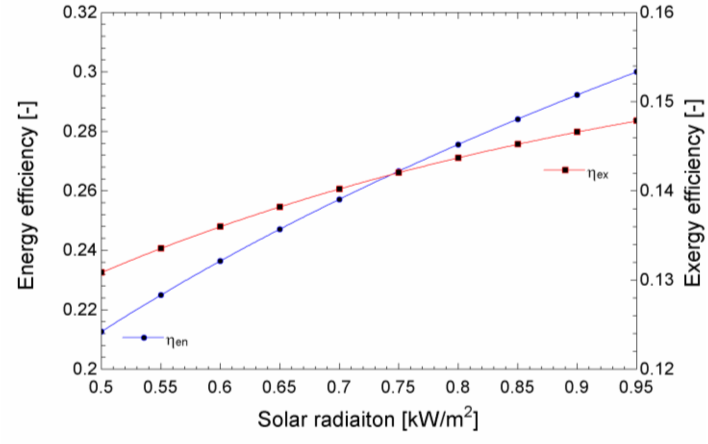

Figure 7. Impact of solar radiation on energetic and exergetic efficiencies of the trigeneration system

It can be seen from these results, the total power generation, refrigerating, and heating rate increase from 21.73 kW to 31.31 kW, from 6.15 to 17.75 kW, and from 10.52 kW to 20.91 kW, respectively, with rising solar intensity.

It is seen in Figure 7 that the energetic and exergetic assessments of the integrated system rise as the solar irradiation increases. Increasing solar irradiation, results in an energy efficiency increase of 42.85 % and exergy performance of 10.69 % for the whole cycle. The reason for this rise is that the increase in the power, refrigerating, and hot water production rates obtained from the trigeneration plant due to the rise in solar radiation.

The behavior of exergy irreversibility with increasing solar intensity is illustrated in Figure 8. As can be seen from the graph, as the solar radiation increases, the exergy destruction of the trigeneration system also increases. This higher irreversibility rate is primarily due to the parabolic collector. The basic reason for this is the heat losses from the collector to the ambient air.

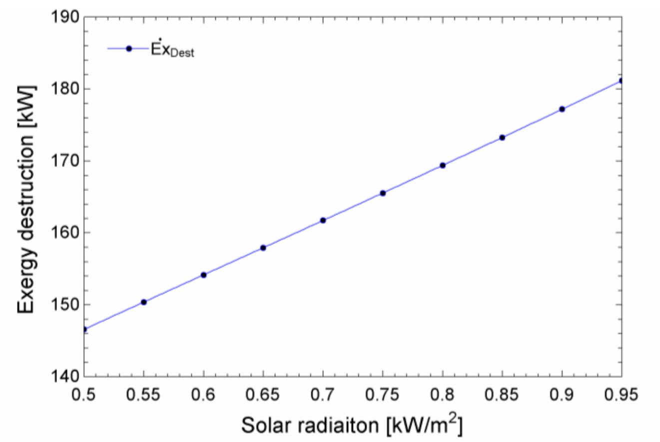

Figure 8. Impact of solar intensity on exergy destruction

Figure 9 demonstrates the variations with the turbine inlet temperature of the power production for the ORC. This diagram shows the increasing tendency in the power generation of the trigeneration system with the increasing turbine inlet temperature. Besides, power generation rises around 42% with an increase in the ORC turbine inlet temperature from 200 °C to 350 °C.

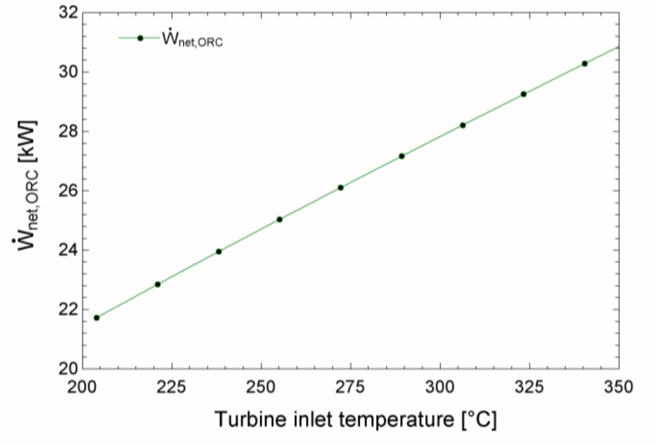

Figure 9. Impact of turbine inlet temperature on power generation

Figure 10 manifests the effect of turbine inlet temperature on the energetic and exergetic assessment of the trigeneration cycle. As can be seen in the figure, as the turbine inlet temperature rises, the energetic and exergetic efficiencies of the trigeneration cycle increase. This is because the power, refrigeration, and hot water capacity, which are the outputs of the trigeneration system, increase as the turbine inlet temperature increases.

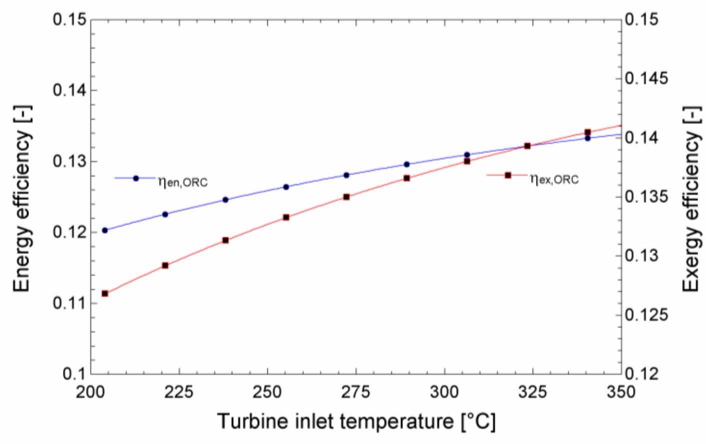

Figure 10. Variation with turbine inlet temperature on energy and exergy efficiencies of the trigeneration system

The variation of the cooling capacity with respect to the generator temperature is given in Figure 11. The refrigeration capacity rises from 8.36 kW to 9.43 kW with a rise in the generator temperature from 70 °C to 120 °C. In the review study of Besagni et al. [43], a comprehensive review was performed on the ejector refrigeration systems. The authors reported that, unsurprisingly, the performance coefficient, so the refrigeration capacity increases with the generator temperature. The results reported in the current study with Figure 11 are in good agreement with this review study. Figure 12 shows the change in the energetic and exergetic efficiencies of the trigeneration system according to the generator temperature. It can be seen from the figure, as the generator temperature rises, the energetic efficiency of the trigeneration system increases while the exergetic efficiency decreases.

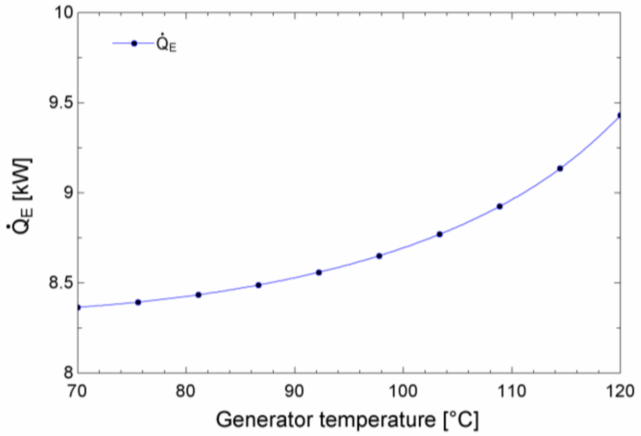

Figure 11. Impact of generator temperature on cooling capacity

According to the results of the initial cost analysis, the investment expenses is calculated to be $108305 using the cost functions tubulated in Table 1. Within the total amount, the cost of the turbine is found to be the most expensive system component with a value of 63690 $ followed by parabolic collectors. Based on the above-mentioned investment costs, the payback period of the integrated system is determined as 4.81 years which is within the acceptable ranges. Mohammadi et al. [33] calculated the payback period of their system to be 1.5 year. The system was consisted of a PTSC driven Rankine cycle integrated with energy storage. Bellos and Tzivanidis [44] investigated an integrated system including Rankine cycle, heating process and refrigeration for building sector.

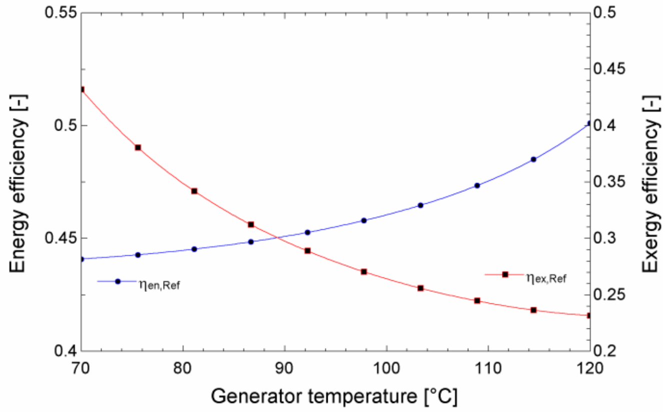

Figure 12. Impact of generator temperature on energetic and exergetic efficiencies of trigeneration system

The system was assisted by solar energy via PTSCs and the payback period was found to be 8.5 years. In another research which was performed by Su [45], the payback period of the PTSC driven integrated system was calculated as 4.39 years.

5. Conclusions

In the study, it is objective to examine the thermodynamic analysis of PTSC supported a novel trigeneration system that can produce power, cooling, and hot water. For this purpose, analyses were performed to define the system performance indicators such as net power production, cooling capacity, energetic, and exergetic efficiencies. In addition, parametric studies were performed to determine the result of solar irradiation, the temperature of the turbine inlet, and generator temperature on system performance. The following are the key conclusions of the study:

- While the power production of the system was determined to be 27.17 kW, the cooling capacity was calculated to be 12.39 kW in the ejector system, and the hot water capacity was calculated to be 16.35 kW.
- The first and second law efficiencies of the ORC were found as 12.96% and 13.66%, while the ejector cooling system COP and exergetic efficiency were calculated as 0.4557% and 27.75%, respectively.
- The overall first and second law efficiencies of the trigeneration system were found to be 26.67% and 14.21%, respectively.
- The parametric results indicated that, as the solar radiation rises, the total power production, cooling, and heating rate increase linearly.
- The rise in solar radiation from 0.5 to 0.95 kW/m^2 resulted in an increase in energy and exergetic efficiencies and irreversibility.
- In addition, the rise in turbine inlet temperature from 200 ℃ to 350 ℃ gives rise to the net power generation of the ORC and first and second law efficiencies of the integrated system.
- When the generator temperature was risen from 70℃ to 120℃, cooling capacity and energy efficiency increased, while exergy efficiency decreased.
- Finally, it was decided that the highest exergy irreversibility rate was in PTSC, with nearly 91% of total irreversibility.
- As the generator temperature was increased from 70℃ to 120℃, cooling capacity and energy efficiency increased, while exergy efficiency decreased.
- It was concluded that the maximum exergy irreversibility rate was in PTSC with nearly 91% of total irreversibility.
- Finally, the payback period of the integrated plant was determined as 4.81 years.

Authors' Contributions

Introduction was written by S.C.T. System Description and Methodology was written by G.S. Thermodynamic analyzes were calculated by OK. Results - Discussion and Conclusions were written all authors.

All authors read and approved the final manuscript.

References

[1] . Al-Hamed, K.H.M., Dincer, I., Investigation of a Concentrated Solar-Geothermal Integrated System with a Combined Ejector-Absorption Refrigeration Cycle for a Small Community, International Journal of Refrigeration, 2019, 106, 407-426.

[2] . Khaliqa, A., Mokheimera, E.M.A., Yaquba, Mohammed., Thermodynamic Investigations on a Novel Solar Powered Trigeneration Energy System, Energy Conversion and Management, 2019, 188, 398-413.

[3] . Haghghi, M.A., Shahriyar, G.H., Seyed, M.P., Chitsaz, A., Talati, F., On the Performance, Economic and Environmental Assessment of Integrating a Solar- Based Heating System with Conventional Heating Equipment; A Case Study, Thermal Science and Engineering, 2019, 100392.

[4] . S.A, Kalogirou., Solar Energy Engineering: Processes and Systems, Second edition, Elsevier, 2013.

[5] . Hachicha, A.A., Rodriguez, I., Capdevila, R., Oliva, A., Heat transfer Analysis and Numerical Simulation of a Parabolic Trough Solar Collector, Applied Energy, 2013, 111, 581-592.

[6] . Alibar, M., Aydin, D., Experimental Analysis of a Parabolic Trough Collector Performance Under Mediterranean Climate Conditions, El-Cezeri Journal of Science and Engineering, 2021, 8(2), 873-886.

[7] . Roy, J.P., Mishra, M.K., Misra, A., Performance Analysis of an Organic Rankine Cycle with Superheating Under Different Heat Source Temperature Conditions, Applied Energy, 2011, 88, 2995–3004.

[8] . Tchanche, B.F, Lambrinos, G., Frangoudakis, A., Papadakis, G., Low-grade Heat Conversion into Power Using Organic Rankine Cycles–A Review of Various Applications, Renewable Sustainable Energy Reviews, 2011, 15(8), 3963–7399.

[9] . European Parliament, Regulation (EC) No 2037/2000 of the European Parliament and of the Council of 29 June 2000 on Substances That Deplete the Ozone Layer, Council of the European Union, 2000.

[10]. United Nations, Kyoto protocol, Kyoto, 1997.

[11]. European Parliament, Regulation (EU) No 517/2017 of the European Parliament and of the Council of 16 April 2014 on Fluorinated Greenhouse Gases and Repealing Regulation (EC) No 842/2006, Council of the European Union, 2014.

[12]. .Ziółkowski, P., Kowalczyk, T., Kornet, S., Badur, J., On Low-Grade Waste Heat Utilization from a Supercritical Steam Power Plant Using an ORC-Bottoming Cycle Coupled with Two Sources of Heat, Energy Conversion Management, 2017, 146, 158–173.

[13]. Shokati, N., Ranjbar, F., Yari, M., Comparative and Parametric Study of Double Flash and Single Flash/ORC Combined Cycles Based on Exergoeconomic Criteria, Applied Thermal Engineering, 2015, 91, 479–495.

[14]. Tashtoush, B.M., Al-Nimr, M.A., Khasawneh, M.A., Comprehensive Review of Ejector Design, Performance and Applications, Applied Energy, 2019, 240, 138–172.

[15]. Taleghani, S.T., Sorin, M., Poncet, S., Nesreddine, H., Performance Investigation of a Two-Phase Transcritical CO_2 Ejector Heat Pump System. Energy Conversion and Management, 2019, 185, 442–454.

[16]. Zheng, B., Weng, Y.W., A Combined Power and Ejector Refrigeration Cycle for Low Temperature Heat Sources, Solar Energy, 2010, 84(5), 784–791.

[17]. Zhang, T., Mohamed, S., Conceptual Design and Analysis of Hydrocarbon-Based Solar Thermal Power and Ejector Cooling Systems in Hot Climates, Journal of Solar Energy Engineering, 2015, 137(2), 021001.

[18]. Khaliq, A., Energetic and Exergetic Performance Investigation of a Solar Based Integrated System for Cogeneration of Power and Cooling, Applied Thermal Engineering, 2017, 112, 1305-1316.

[19]. Eisavi, B., Khalilarya, S., Chitsaz, A., Rosen, M.A., Thermodynamic Analysis of a Novel Combined Cooling, Heating and Power System Driven by Solar Energy, Applied Thermal Engineering, 2018, 129, 1219–1229.

[20]. Al-Sulaiman, F.A., Hamdullahpur, F., Dincer, I, Performance Assessment of a Novel System Using Parabolic Trough Solar Collectors for Combined Cooling, Heating and Power Production, Renewable Energy, 2012, 48, 161-172.

[21]. Al-Sulaiman, F.A, Dincer, I., Hamdullahpur, F., Exergy Modeling of a New Solar Driven Trigeneration System, Solar Energy, 2011, 85(9), 2228-2243.

[22]. Moghimi, M., Emadi, M., Ahmadi, P., Moghadasi, H., 4E Analysis and Multi-Objective Optimization of a CCHP Cycle Based on Gas Turbine and Ejector Refrigeration, Applied Thermal Engineering, 2018, 141, 516–530.

[23]. Mosaffa, A.H., Farshi, L.G., Thermodynamic and Economic Assessments of a Novel CCHP Cycle Utilizing Low-Temperature Heat Sources for Domestic Applications, Renewable Energy, 2018, 120, 134–150.

[24]. Kheiri, R., Ghaebi, H., Ebadollahi, M., Rostamzadeh, H., Thermodynamic Modeling and Performance Analysis of Four New Integrated Organic Rankine Cycles (A Comparative Study), Applied Thermal Engineering, 2017, 122, 103–117.

[25]. Gupta, D.K., Kumar, R., Kumar, N., Performance Analysis of PTC Field Based Ejector Organic Rankine Cycle Integrated with a Triple Pressure Level Vapor Absorption System (EORTPAS), Engineering Science and Technology, an International Journal, 2020, 23, 82–91.

[26]. Khaliq, A., Kumar, R., Mokheimer E.M.A., Investigation on a Solar Thermal Power and Ejector-Absorption Refrigeration System Based on First and Second Law Analyses, Energy, 2018, 164, 1030-1043.

[27]. Elakhdar, M., Landoulsi, H., Tashtoush, B., Nehdi, E., Kairouani, L., A Combined Thermal System of Ejector Refrigeration and Organic Rankine Cycles for Power Generation Using a Solar Parabolic Trough, Energy Conversion and Management, 2019, 199, 111947.

[28]. Klein SA. Engineering Equation Solver (EES). F-Chart, 2021.

[29]. Kizilkan, O., Khanmohammadi, S., Saadat-Targhi, M, Solar Based CO_2 Power Cycle Employing Thermoelectric Generator and Absorption Refrigeration: Thermodynamic Assessment and Multi-objective Optimization. Energy Convers Management, 2019, 200, 112072.

[30]. Dincer, I., Rosen, M.A, Exergy: Energy, Environment and Sustainable Development. 1st edition., Elsevier Science, Oxford, UK, 2007.

[31]. Kotas, T.J., The Exergy Method of Thermal Plant Analysis, Butter-Worths, London, UK, 1985.

[32]. Tiwari, G.N., Solar Energy Fundamentals Design Modelling and Applications, 2002.

[33]. Mohammadi, A., Ahmadi, M.H., Bidi, M., Ghazvini, M., Ming ,T., Exergy and Economic Analyses of Replacing Feedwater Heaters in a Rankine Cycle with Parabolic Trough Collectors, Energy Reports, 2018, 4, 243-251.

[34]. Habibi, H., Zoghi, M., Chitsaz, A., Javaherdeh, K., Ayazpour, M., Thermo-Economic Performance Comparison of Two Configurations of Combined Steam and Organic Rankine Cycle with Steam Rankine Cycle Driven by Al_2O_3-Therminol VP-1 Based PTSC, Solar Energy, 2019, 180, 116-132.

[35]. Shokati, N., Ranjbar, F., Yari, M., Exergoeconomic Analysis and Optimization of Basic, Dual-Pressure and Dual-Fluid ORCs and Kalina Geothermal Power Plants: A Comparative Study, Renewable Energy, 2015, 83, 527-542.

[36]. Nazari N., Heidarnejad, P., Porkhial, S., Multi-Objective Optimization of a Combined Steam-Organic Rankine Cycle Based on Exergy and Exergo-Economic Analysis for Waste Heat Recovery Application, Energy Conversion Management, 2016, 127, 366-379.

[37]. Ahmadi, P., Modeling, Analysis and Optimization of Integrated Energy Systems for Multigeneration Purposes, PhD thesis, University of Ontario Institute of Technology, Faculty of Engineering and Applied Science, Oshawa, Ontario, Canada, 2013.

[38]. Khanmohammadi, S., Musharavati, F., Kizilkan, F., Nguyen, D.D., Proposal of a New Parabolic Solar Collector Assisted Power-Refrigerationsystem Integrated with Thermoelectric Generator Using 3E analyses: Energy,exergy, and Exergo-Economic, Energy Conversion Management, 2020, 220, 113055.

[39]. Kajurek, J., Rusowicz, A., Grzebielec, A., Bujalski, W., Futyma, K., Rudowicz, Z., Selection of refrigerants for a modified organic Rankine cycle, Energy, 2019, 168, 1-8.

[40]. Koc, M., Tukenmez, N., Ozturk. M., Development and Thermodynamic Assessment of a Novel Solar and Biomass Energy Based Integrated Plant for Liquid Hydrogen Production, International Journal of Hydrogen Energy, 2020, 45, 34587-34607.

[41]. Yamaguchi, H., Yamasaki, H., Kizilkan, O., Experimental investigation of solar-assisted transcritical CO_2 Rankine cycle for summer and winter conditions from exergetic point of view, Int J Energy Res., 2020, 44, 1189–1102.

[42]. PVGIS, Joint Research Centre (JRC) of European Union https://ec.europa.eu/jrc/en/pvgis. Date of Access: 27.10.2021.

[43]. Besagni, G., Mereu, R., Inzoli, F., Ejector refrigeration: A comprehensive review, Renewable and Sustainable Energy Reviews, 2016, 53, 373-407.

[44]. Bellos, E., Tzivanidis, C., Parametric Analysis of a Solar-Driven Trigeneration System with an Organic Rankine Cycle and a Vapor Compression Cycle, Energy and Built Environment, 2021, 2(3), 278-289.

[45]. Su, D., Comprehensive Thermodynamic and Exergoeconomic Analyses and Multi-Objective Optimization of a Compressed Air Energy Storage Hybridized with a Parabolic Trough Solar Collectors, Energy, 2021, 122568.